NANO LETTERS

Letter

pubs.acs.org/NanoLett

High-Performance All-Solid-State Lithium–Sulfur Battery Enabled by a Mixed-Conductive Li_2S Nanocomposite

Fudong Han, Jie Yue, Xiulin Fan, Tao Gao, Chao Luo, Zhaohui Ma, Liumin Suo, and Chunsheng Wang*

Department of Chemical and Biomolecular Engineering, University of Maryland, College Park, Maryland, 20742, United States

Supporting Information

ABSTRACT: All-solid-state lithium–sulfur batteries (ASSLSBs) using highly conductive sulfide-based solid electrolytes suffer from low sulfur utilization, poor cycle life, and low rate performance due to the huge volume change of the electrode and the poor electronic and ionic conductivities of S and Li_2S. The most promising approach to mitigate these challenges lies in the fabrication of a sulfur nanocomposite electrode consisting of a homogeneous distribution of nanosized active material, solid electrolyte, and carbon. Here, we reported a novel bottom-up method to synthesize such a nanocomposite by dissolving Li_2S as the active material, polyvinylpyrrolidone (PVP) as the carbon precursor, and Li_6PS_5Cl as the solid electrolyte in ethanol, followed by a coprecipitation and high-temperature carbonization process. Li_2S active material and Li_6PS_5Cl solid electrolyte with a particle size of ~4 nm were uniformly confined in a nanoscale carbon matrix. The homogeneous nanocomposite electrode consisting of different nanoparticles with distinct properties of lithium storage capability, mechanical reinforcement, and ionic and electronic conductivities enabled a mechanical robust and mixed conductive (ionic and electronic conductive) sulfur electrode for ASSLSB. A large reversible capacity of 830 mAh/g (71% utilization of Li_2S) at 50 mA/g for 60 cycles with a high rate performance was achieved at room temperature even at a high loading of Li_2S (~3.6 mg/cm^2). This work provides a new strategy to design a mechanically robust, mixed conductive nanocomposite electrode for high-performance all-solid-state lithium sulfur batteries.

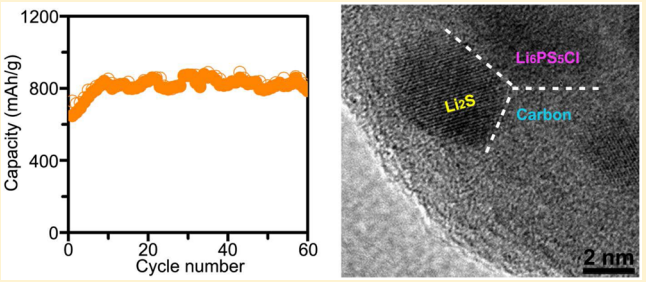

KEYWORDS: *All-solid-state, lithium–sulfur batteries, nanocomposite, mixed-conductive, electrode, reinforcement*

All-solid-state lithium–sulfur batteries (ASSLSBs) are attracting intense research interest because of several advantages: (1) the inherent high energy of lithium–sulfur chemistry and the abundance of sulfur,[1,2] (2) the improvement of safety by using nonflammable inorganic solid electrolyte, and (3) the increase of energy efficiency due to the elimination of polysulfide shuttle.[3−5] Despite these great promises, the performance of ASSLSBs is still far worse than the liquid–electrolyte lithium–sulfur batteries in terms of sulfur utilization, cycling, and rate performances, even though sulfide-based solid electrolytes with a comparable ionic conductivity as liquid electrolytes were used.[6−8] The poor performance of ASSLSBs could be mainly ascribed to two main challenges.

First, the poor electronic and ionic conductivities of sulfur and its discharge product require S (or Li_2S) has to be uniformly distributed in a high and balanced ionic/electronic conducting matrix. Inspired by the success of liquid-electrolyte lithium–sulfur battery, considerable engineering efforts have been done to improve the electronic conductivity of sulfur cathode for ASSLSB by incorporating a variety of electronic conductive materials like copper,[6,9] acetylene black,[10] carbon nanofibers,[11] graphite,[12] and mesoporous carbon.[13] However, only limited improvement on enhancing the sulfur utilization and rate performance of these ASSLSBs have been achieved. Therefore, simply increasing the electronic conductivity cannot guarantee a high-performance ASSLSB because the charge/discharge of the electrode also requires the facile transport of lithium ions. As a matter of fact, the enabling of the facile ion transport is more critical in all-solid-state batteries since solid electrolytes are not infiltrative as liquid electrolytes. The most recent work indicate that the increase of ionic conductivity of the electrode could effectively improve the electrochemical performance of solid state batteries.[14,15] Moreover, a balanced ionic conductivity with the electronic conductivity is much more difficult to be achieved in ASSLSBs than in liquid electrolyte Li-ion batteries where the porosity, pore size, and distribution in the electrodes can be simply engineered to tune the ionic conductivity of the electrodes since liquid electrolyte will be infiltrated into the pores. For instance, a dual-scale porous electrode in which accessible porosity is distributed at multiple scales was reported to improve the ionic transport in the thick $LiCoO_2$ electrode for liquid–electrolyte battery.[16] In order to improve the ionic conductivity of the electrodes, several lithium superionic sulfides were fabricated as cathodes for ASSLSBs.[17−19] Despite great cycling stability (>100 cycles), these batteries have to be operated at 60 °C even at a low

Received: April 29, 2016
Revised: June 13, 2016
Published: June 20, 2016

DOI: 10.1021/acs.nanolett.6b01754
Nano Lett. 2016, 16, 4521–4527

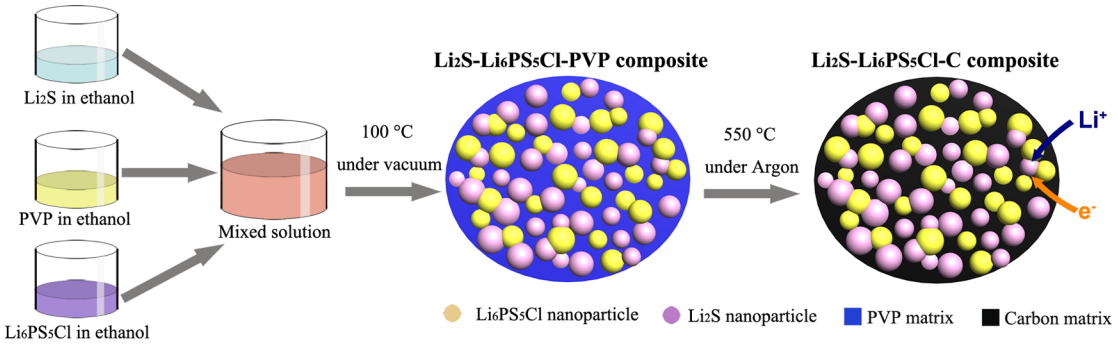

Figure 1. Schematic illustration of the bottom-up synthesis of the mixed conducting Li_2S nanocomposite.

loading of active material (0.25−0.60 mg/cm^2).[17,18] The above-mentioned reports indicated that the improvement of only one conductivity, either electronic or the ionic conductivity, cannot achieve the high performance of ASSLSB in terms of sulfur utilization and rate capability. Therefore, both electronic and ionic conductivities of the sulfur electrode should be improved and balanced. In addition, the intrinsic poor ionic and electronic conductivity of S and Li_2S also implies that the active material should be in nanosize to shorten the diffusion distances for both Li^+ and electrons, and this would become more important for the solid state cells because of the absence of the dissolved electrode (which is present in the liquid−electrolyte lithium sulfur batteries) that could facilitate the diffusion and reaction kinetics.[3] On the other hand, the nanosized S (or Li_2S) would require an electronic/ionic conducting network in the same nanometer scale to achieve its maximum utilization. However, no such work has been reported on simultaneously improving the ionic and electronic conductivity of sulfur cathodes at nanoscale for ASSLSBs.

The second challenge arises from the huge stress within the sulfur electrode in the ASSLSBs because of the large volume change (76%) during lithiation/delithiation. Unlike the liquid electrolyte lithium−sulfur battery where the flowable liquid electrolyte infiltrated in the pores of electrodes (porosity ∼30 vol %) can effectively accommodate the volume change, sulfur electrodes in ASSLSB typically consisted of a thick, dense composite of active material, solid electrolyte, and electronic conductive additives. The large volume changes of the sulfur electrode during lithiation/delithiation are highly constrained by the rigid solid electrolytes, resulting in a huge strain/stress at the electrode/electrolyte interface. The huge strain/stress generated during the charge/discharge process could easily exceed the fracture toughness of S (or Li_2S), leading to the formation of cracks within the active material. It should be noted that the cracks have even been observed in the oxide cathode particles with a very small volume change (<7%) during lithiation/delithiation in the commercialized liquid−electrolyte lithium ion batteries where high porosity of the cathode also helped to release partial stress.[20−22] In the liquid−electrolyte cells, the liquid electrolytes can infiltrate into the crack to maintain the Li-ion conductive pathway although the electronic conduction is reduced. However, the crack formed in the electrode of a solid state cell will make the active material detach from the solid electrolyte and/or carbon, losing the ionic/electronic conduction and thus leading to fast capacity decay. Therefore, how to get a mechanically robust sulfur composite cathode is critical to achieve a long-cycling all-solid-state lithium sulfur battery, but unfortunately, there are still no reports to address this specific issue.

The utilization of hard nanoparticles to reinforce the soft matrix materials (e.g., polymer,[23] metal[24]) has been widely reported because the formed nanocomposite demonstrated a dramatically improved mechanical strength such as ductility and toughness. The mechanical strength of the formed nanocomposite could be further enhanced if the reinforcing nanoparticles are in situ grown within the soft matrix.[23] Therefore, the mechanical property of the sulfur electrode composite for all-solid-state batteries could be largely improved if the nanosized active material and solid electrolyte particles as the reinforcement phases can be in situ grown in the carbon matrix to make a nanocomposite electrode. The improvement on the mechanical property of the electrode nanocomposite would be expected to improve the cycling life of the battery. In addition, a high utilization of sulfur (high capacity) could also be expected for the nanocomposite electrode because of the intimate and sufficient triple-phase contact of the active material, solid electrolytes and carbon.[25,26] Another fascinating advantage of the nanocomposite electrode is that the nanoscale percolating network for both lithium ions and electrons could be easily formed because of the uniform distribution of nanoscale ionic conductive solid electrolytes and electronic conductive carbon. In addition, the mixed-conductive network in the nanocomposite electrode could also reduce the amount of solid electrolyte in the electrode, while still maintaining the sufficient contact between electrolyte and electrode.[15] Therefore, the fabrication of a nanocomposite sulfur electrode is the most promising direction to achieve a high-performance ASSLSB based on the simultaneous improvement on the mechanical property, ionic conductivity and electronic conductivity of sulfur cathode. However, it is very challenging to synthesize a nanocomposite with uniform distribution of the three components (carbon, active material, solid electrolyte) at nanoscale. High-energy ball-milling was used to prepare the composite electrode for all-solid-state lithium sulfur battery.[27] Despite the simple and scalable approach, the ball-milling process cannot guarantee all the particles of these three components are within nanometer size and uniformly distributed because of the different properties of these components.[7]

Herein, we proposed a novel bottom-up approach to prepare the Li_2S nanocomposite by dissolving Li_2S as the active material, polyvinylpyrrolidone (PVP) as the carbon precursor, and Li_6PS_5Cl as the solid electrolyte in ethanol, followed by a coprecipitation and high-temperature carbonization process. Using prelithiated (or pre-expanded) Li_2S as the cathode could provide enough space for the volume change of the electrode during lithiation/delithiation. A uniform, nanoscale mixing of active material, solid electrolyte, and carbon will be achieved

DOI: 10.1021/acs.nanolett.6b01754
Nano Lett. 2016, 16, 4521−4527

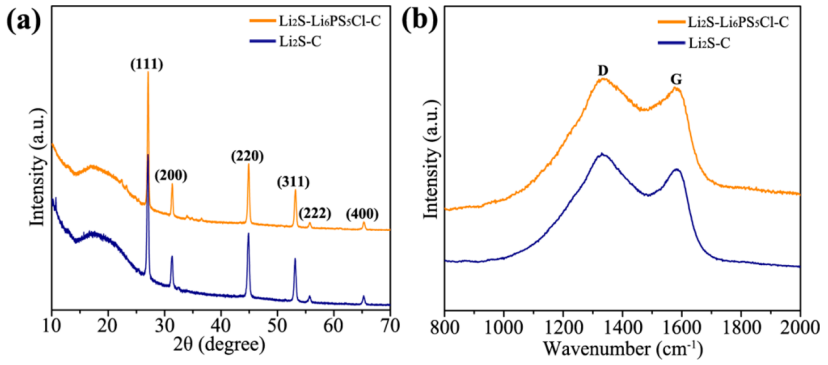

Figure 2. X-ray diffraction patterns (a) and Raman spectra (b) of the as-obtained Li_2S−Li_6PS_5Cl−C and Li_2S−C composites.

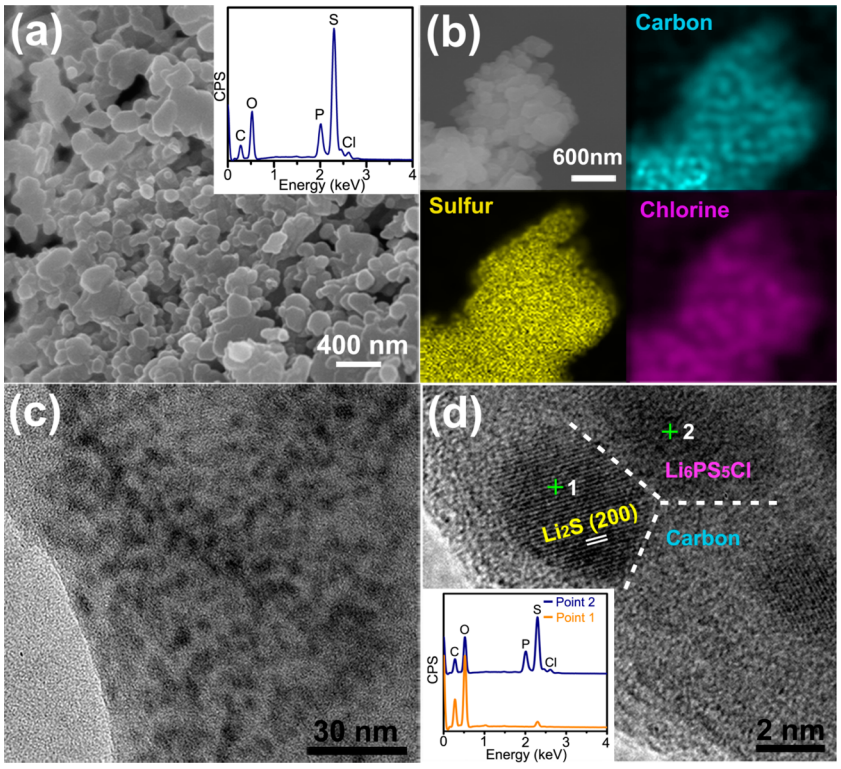

Figure 3. (a) SEM image of the as-obtained Li_2S−Li_6PS_5Cl−C nanocomposite. The inset shows the EDS result. (b) The elemental mappings of carbon, sulfur and chlorine in the composite. (c) The TEM image of the Li_2S−Li_6PS_5Cl−C nanocomposite. (d) The high-resolution TEM image of the as-obtained Li_2S−Li_6PS_5Cl−C nanocomposite, and the inset shows the EDS results at point 1 and point 2, respectively.

from the bottom up approach. The significantly improved mechanical and mixed conducting properties of the Li_2S nanocomposite electrode enabled an excellent room-temperature electrochemical performance of all-solid-state lithium battery.

Figure 1 shows a schematic illustration for the bottom up synthesis of the Li_2S nanocomposite. First, Li_2S as the active material, PVP as the carbon precursor, and Li_6PS_5Cl ($\sigma_{Li} \sim 10^{-3}$ S/cm)[28,29] as the solid electrolyte were dissolved in the anhydrous ethanol separately. Li_6PS_5Cl was selected as the electrolyte additive because it is the only reported sulfide-based solid electrolyte that can be dissolved in ethanol which could also dissolve Li_2S and PVP.[30] The weight ratio of Li_2S, PVP, and Li_6PS_5Cl is 2:2:1. Recent work indicates that Li_2S is stable during the high temperature carbonization process of PVP,[31] and the structure and the ionic conductivity of Li_6PS_5Cl will not change largely after its dissolution and precipitation in ethanol.[30] These solutions were then mixed together, and no apparent precipitation could be observed. The mixed solution was then dried at 100 °C under vacuum to evaporate the ethanol. Because of the affinity between the polar precipitates (Li_2S, Li_6PS_5Cl) and high polarity functional groups in PVP, nanoparticles of Li_2S and Li_6PS_5Cl will be coated with PVP during the evaporation process to form a Li_2S−Li_6PS_5Cl−PVP composite.[31] The obtained nanocomposite was then heated at 550 °C under argon atmosphere to carbonize PVP, and then Li_2S−Li_6PS_5Cl−C nanocomposite was formed with the Li_2S and Li_6PS_5Cl nanoparticles distributed in carbon matrix. The uniform, nanoscale mixing of Li_2S, Li_6PS_5Cl and carbon in the composite could enable facile transports for both lithium ions and electrons, making the Li_2S−Li_6PS_5Cl−C nanocomposite an excellent mixed conducting electrode. A Li_2S−C nanocomposite was also prepared as a control sample using the

DOI: 10.1021/acs.nanolett.6b01754
Nano Lett. 2016, 16, 4521−4527

same procedure without adding Li_6PS_5Cl in the original solution.

Figure 2a shows the XRD patterns of as-obtained Li_2S–Li_6PS_5Cl–C and Li_2S–C composites. The main peaks of both composites could be well indexed to the (111), (200), (220), (311), (222), and (400) of Li_2S (JCPDS: 65-2981). The broad peak around 18 degree is attributed to the airtight sample holder for the XRD test. No impurities could be observed in the XRD of two nanocomposites. The XRD pattern of crystal Li_6PS_5Cl is shown in Figure S1 of SI. The absence of the peaks of Li_6PS_5Cl is possibly because of the low crystallinity of Li_6PS_5Cl compared with Li_2S. Raman spectra of the as-obtained Li_2S–Li_6PS_5Cl–C and Li_2S–C composites were shown in Figure 2b. Two characteristic peaks around 1330 and 1590 cm^{-1} could be ascribed to the D band and G band of graphitic carbon, respectively, indicating the presence of carbon in the nanocomposite.

Figure 3a shows the SEM image of the as-obtained Li_2S–Li_6PS_5Cl–C nanocomposite, which consists of irregular particles with particle sizes of 100–500 nm. Energy dispersive spectroscopy (EDS) analysis (inset of Figure 3a) confirms the presence of carbon, oxygen, phosphorus, sulfur, and chlorine in the composite, and the observed oxygen may be caused by the reaction between sulfides and air during the sample transfer for the SEM test. The EDS analysis from multiple positions indicates that the average content of carbon in the nanocomposite is about 10.6 wt % (Figure S2 of SI). Since the weight ratio between Li_2S and Li_6PS_5Cl is 2:1, after carbonization the ratio of carbon, Li_2S, Li_6PS_5Cl in the nanocomposite is 10.6:59.6:29.8. Therefore, the weight content of Li_2S active material in the Li_2S–Li_6PS_5Cl–C nanocomposite is 59.6 wt %. In addition, the content of Li_2S in the Li_2S–C nanocomposite was also determined to be 85.7 wt % from the EDS results. The uniform distribution of carbon, sulfur, and chlorine from the elemental mappings (Figure 3b) implies that Li_2S, Li_6PS_5Cl, and carbon are uniformly distributed within the composites. High-resolution TEM was used to reveal the distribution of these components. Figure 3c shows that the 100–500 nm particles observed from SEM in Figure 3a are composed of a large amount of ~4 nm particles distributed in carbon matrix. The lattice spacing of the nanocrystallite shown in the high magnification TEM image (Figure 3d) is determined to be 0.27 nm, close to the *d*-spacing (0.28 nm) of the (200) plane of Li_2S. The result indicates that the nanocrystallites could be ascribed to Li_2S, and this is also supported by the EDS result of point 1 shown in the inset of Figure 3d. In addition, nanoparticles with a lower crystallinity can also be observed in the composite, which is ascribed to Li_6PS_5Cl solid electrolyte based on the higher content of phosphorus and chlorine in the EDS result of point 2 (inset of Figure 3d). The low crystallinity of Li_6PS_5Cl is also consistent with the absence of XRD peaks.

To confirm the mixed conductive property of the Li_2S–Li_6PS_5Cl–C nanocomposite, the electronic and ionic conductivities of the as-obtained nanocomposites at room temperature were measured. The electronic conductivity was measured by a four-probe method using the pressed pellet of the nanocomposites, while the ionic conductivity was measured by the electrochemical impedance spectra (EIS) test of the electron-blocking $Pt/Li_{10}GeP_2S_{12}$/nanocomposite/$Li_{10}GeP_2S_{12}$/Pt cell. $Li_{10}GeP_2S_{12}$ electrolyte was used to block the electron transport so that the measured impedance is solely from Li^+. The conductivity data are summarized in Table 1.

Table 1. Electronic and Ionic Conductivities of the Li_2S–C and Li_2S–Li_6PS_5Cl–C Nanocomposites at Room Temperature

samples	electronic conductivity	ionic conductivity
Li_2S	~10^{-13} S/cm[8]	~10^{-9} S/cm[32]
Li_2S–C	5.6×10^{-5} S/cm	6.3×10^{-10} S/cm
Li_2S–Li_6PS_5Cl–C	2.2×10^{-5} S/cm	9.6×10^{-6} S/cm

Compared with pure Li_2S, a dramatic increase of the electronic conductivity (from 10^{-13} S/cm to 10^{-5} S/cm) has been achieved for both Li_2S–C and Li_2S–Li_6PS_5Cl–C nanocomposites, indicating that the introduction of carbon could effectively increase the electronic conductivity of cathode. However, the introduction of carbon cannot largely improve the ionic conductivity of Li_2S,[33] which can be reflected by the poor ionic conductivity of the Li_2S–C composite (6.3×10^{-10} S/cm). The Li_2S–Li_6PS_5Cl–C nanocomposite, on the other hand, exhibits a 3 orders of magnitude increase in ionic conductivity (from 10^{-9} S/cm of Li_2S to 9.6×10^{-6} S/cm of Li_2S–Li_6PS_5Cl–C). The typical EIS of the $Pt/Li_{10}GeP_2S_{12}$/nanocomposite/$Li_{10}GeP_2S_{12}$/Pt cell is shown in Figure S3 of SI. The high ionic conductivity of the Li_2S–Li_6PS_5Cl–C nanocomposite indicates that the Li_6PS_5Cl in the nanocomposite with a low crystallinity is also a fast Li^+ conductor, implying that the crystallinity does not have a significant effect on the ionic conductivity of Li_6PS_5Cl. The ionic conductivity of Li_2S–Li_6PS_5Cl–C nanocomposite is comparable with that of the reported lithium superionic sulfide cathodes.[17,18] However, unlike the electron-insulating lithium superionic sulfides, the Li_2S–Li_6PS_5Cl–C nanocomposite also has a very high electronic conductivity. It should also be noted that electronic conductivity of the Li_2S–Li_6PS_5Cl–C nanocomposite is only about two times higher than its ionic conductivity, indicating a well-balanced electronic and ionic conductivity. The HRTEM and conductivity measurement confirm that the uniform, nanoscale distribution of Li_2S, Li_6PS_5Cl, and carbon within the composite could effectively improve both the electronic conductivity and the ionic conductivity of the material, enabling the Li_2S–Li_6PS_5Cl–C nanocomposite to be an excellent electrode for ASSLSBs.

The electrochemical performances of the Li_2S–C and Li_2S–Li_6PS_5Cl–C as the cathodes for ASSLSBs were examined using $80Li_2S{\cdot}20P_2S_5$ glass ceramic as the solid electrolyte and Li–In alloy as the anode. To improve the kinetics of the electrode with the high mass loading, additional electronic-conductive additive (carbon black) and ionic-conductive additive ($80Li_2S{\cdot}20P_2S_5$ glass-ceramic) were mixed with the nanocomposite to form multiscale electronic/ionic conducting networks in the electrode composite. The content of the Li_2S active material in the whole cathode composite is 36 wt %, which is much larger than the previous reported values.[7,9,27,34] The $80Li_2S{\cdot}20P_2S_5$ glass ceramic was used as the solid electrolyte in the composite electrode and in the all-solid-state Li–S battery because its ionic conductivity (1.3×10^{-3} S/cm)[35] is about three times larger than that of the Li_6PS_5Cl solid electrolyte (4×10^{-4} S/cm).[29] The utilization of Li–In alloy as anode could help to reduce the interfacial resistance/instability at the anode/electrolyte interface by suppressing the detrimental decomposition of solid electrolyte, although a sacrifice of voltage output also exists.[36] Figure 4a shows the thermodynamically equilibrium voltage curves of the Li_2S–C and Li_2S–Li_6PS_5Cl–C electrodes obtained by a galvanostatic intermittent titration

DOI: 10.1021/acs.nanolett.6b01754
Nano Lett. 2016, 16, 4521–4527

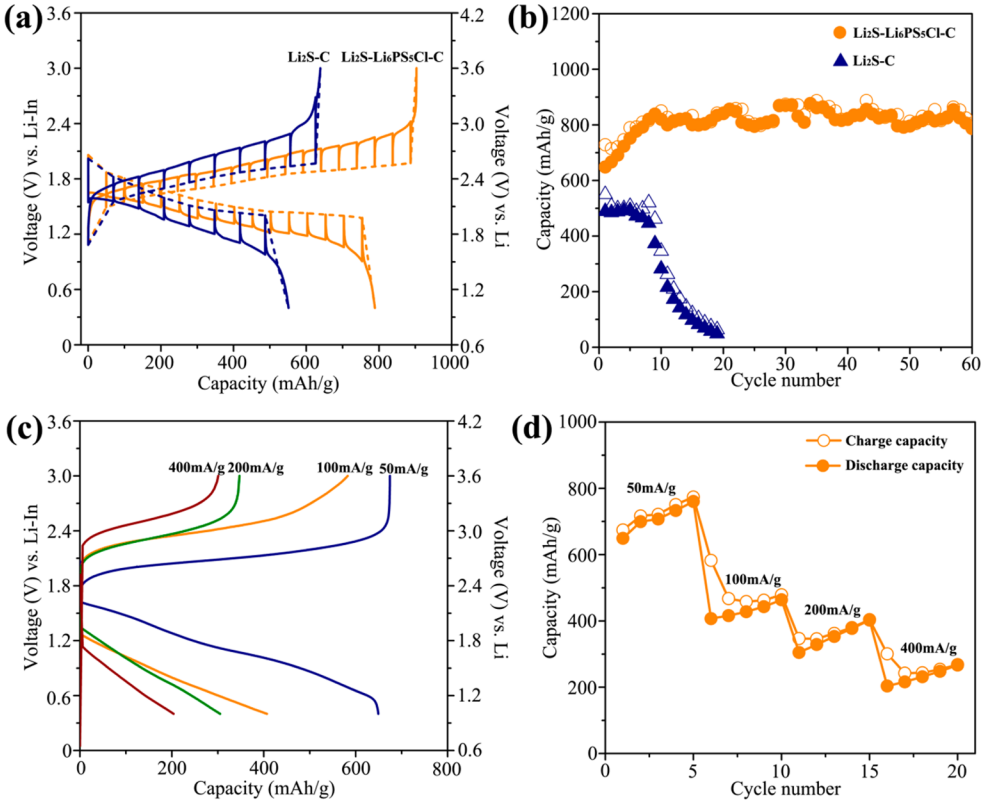

Figure 4. (a) Equilibrium (open-circuit)−voltage (dashed lines) and transient voltage (solid lines) profiles versus capacity for the 1st cycle of the Li_2S−C and Li_2S−Li_6PS_5Cl−C nanocomposite electrodes. Both electrodes were tested at a current density of 50 mA/g. (b) Cycling performances of the Li_2S−C and Li_2S−Li_6PS_5Cl−C nanocomposite electrodes at 50 mA/g. (c) Charge/discharge profiles of the Li_2S−Li_6PS_5Cl−C nanocomposite electrode at various current densities from 50 mA/g to 400 mA/g. Note that four fresh all-solid-state cells were tested under different current densities, and the first cycle charge/discharge curves were provided. (d) Rate performance of the Li_2S−Li_6PS_5Cl−C nanocomposite electrode. All of the current densities and capacities were calculated based on the weight of Li_2S. The loading of the Li_2S is about 3.6 mg/cm^2. All of the tests were performed at room temperature.

technique (GITT). Unlike the charge/discharge behaviors of Li_2S−C and Li_2S−Li_6PS_5Cl−C electrodes in the liquid electrolyte (Figure S4 of SI) with two characteristic plateaus representing two reduction processes from solid sulfur to liquid high-order polysulfides, and from liquid high-order polysulfides to solid Li_2S, respectively,[37,38] only one plateau could be observed for both Li_2S−C and Li_2S−Li_6PS_5Cl−C electrodes. This indicates that only a binary solid−solid phase transition (between Li_2S and S) occurs during the charge/discharge of the nanocomposite electrodes in all-solid-state batteries, which is consistent with the previous reports.[7,27,39] The higher capacity of Li_2S−Li_6PS_5Cl−C than that of Li_2S−C demonstrates that the high and mixed ionic/electronic conductivity can enhance the utilization of Li_2S in the electrode. In addition to the thermodynamically equilibrium potentials, the Li_2S−Li_6PS_5Cl−C electrode also has a smaller overpotential (the difference between charge/discharge potential and the equilibrium potential) than that of Li_2S−C as demonstrated in GITT measurement in Figure 4a. Therefore, Li_2S−Li_6PS_5Cl−C electrode has a lower reaction resistance than the Li_2S−C electrode, indicating that the mixed conducting nanocomposite could also help to improve the kinetics of the electrode during charge and discharge process.

Figure 4b compares the cycling performance of the Li_2S−C and Li_2S−Li_6PS_5Cl−C electrodes measured at the current density of 50 mA/g. The Li_2S−C electrode exhibits a low reversible capacity of 489 mA h/g for the first cycle. The capacity quickly decays after 10 cycles and drops to 49 mA h/g at the 20th cycle. However, a much higher initial capacity of 648 mA h/g was delivered by the Li_2S−Li_6PS_5Cl−C electrode. The capacity gradually increases for the first few cycles and then stabilizes at about 830 mA h/g for 60 cycles. The excellent cycling stability is a significant advance compared with the previous reports with a limited cycle number (<20).[7,9,27,34,39] The increase of the capacity for the initial cycles is due to the activation process, as confirmed by continuously decreased resistances from the EIS test (Figure S5 of SI). Even with the higher content of active material in the Li_2S−Li_6PS_5Cl−C nanocomposite electrode, the utilization of Li_2S (the ratio of the real capacity to the theoretical capacity) is 71%, which is higher than the previous work with similar loading of Li_2S (3.6 mg/cm^2).[7,9,27,34] Figure 4c shows the charge/discharge curves of the Li_2S−Li_6PS_5Cl−C electrode at different current densities in the first cycle. The result indicates that the Li_2S−Li_6PS_5Cl−C electrode was able to charge/discharge at a high current density up to 400 mA/g. Reversible capacities of 648 mA h/g, 407 mA h/g, 304 mA h/g, and 202 mA h/g could be achieved at the current densities of 50 mA/g, 100 mA/g, 200 mA/g, and 400 mA/g, respectively, demonstrating the excellent rate performance of the Li_2S−Li_6PS_5Cl−C electrode (Figure 4d).

The exceptional electrochemical performance of the Li_2S−Li_6PS_5Cl−C nanocomposite in terms of utilization of Li_2S, cycling, and rate performances makes it a promising candidate as the cathode for ASSLSBs. Such pronounced electrochemical

DOI: 10.1021/acs.nanolett.6b01754
Nano Lett. 2016, 16, 4521−4527

performance can be ascribed to the unique nanocomposite structure of Li_2S–Li_6PS_5Cl–C. First, the in situ grown hard Li_2S and Li_6PS_5Cl nanoparticles as reinforcement phases in the soft and nanoscale carbon matrix could help to buffer the strain/stress generated during the delithiation/lithiation process, beneficial to the cycling performance. In addition, the uniform, nanoscale distribution of Li_2S, Li_6PS_5Cl and C in the composite could provide large triple-phase contact for the charge transfer reaction of Li_2S, leading to a high utilization of the active material. Meanwhile, the mixed conducting property of the Li_2S–Li_6PS_5Cl–C nanocomposite enables the facile transport of both lithium ions and electrons through a nanoscale percolating network, contributing to a high rate performance.

In summary, a mixed conducting Li_2S nanocomposite was prepared via a simple bottom-up method by dissolving Li_2S, Li_6PS_5Cl, and PVP in the same solvent followed by the coprecipitation and high-temperature carbonization process. Nanosized Li_2S and Li_6PS_5Cl with particle size around 4 nm were homogeneously distributed in the carbon matrix, forming a secondary particle with size of 100–500 nm. The nanoscale and uniform distribution of the Li_2S, Li_6PS_5Cl, and carbon enabled a great improvement on the mechanical and mixed-conducting properties of the electrode. All-solid-state lithium sulfur battery using the Li_2S–Li_6PS_5Cl–C nanocomposite as cathode delivered a large reversible capacity (830 mA h/g for 60 cycles at 50 mA/g) and excellent rate performance at room temperature. The simple approach offers a new pathway for large-scale production of the cathode material for high performance ASSLSBs. The result could also provide valuable guidelines to develop other mixed-conducive electrodes for all-solid state lithium batteries.

■ ASSOCIATED CONTENT

Supporting Information

The Supporting Information is available free of charge on the ACS Publications website at DOI: 10.1021/acs.nanolett.6b01754.

Details of experimental methods, characterizations, electrochemistry, and additional figures (Figures S1–S5) (PDF)

■ AUTHOR INFORMATION

Corresponding Author

*E-mail: cswang@umd.edu.

Notes

The authors declare no competing financial interest.

■ ACKNOWLEDGMENTS

The authors thank Prof. Gary Rubloff and Chanyuan Liu for the help on the electronic conductivity measurement. This work was supported by Army Research Office (Program Manager: Dr. Robert Mantz) under Award No. W911NF1510187 and National Science Foundation under Award No. 1235719. The authors also thank Mr. Rui Liu from Xiamen University for the kind help on the figure plot.

■ REFERENCES

(1) Ji, X.; Lee, K. T.; Nazar, L. F. *Nat. Mater.* **2009**, *8*, 500–506.
(2) Manthiram, A.; Fu, Y.; Chung, S. H.; Zu, C.; Su, Y. S. *Chem. Rev.* **2014**, *114*, 11751–11787.
(3) Mikhaylik, Y. V.; Akridge, J. R. *J. Electrochem. Soc.* **2004**, *151*, A1969–A1976.
(4) Hassoun, J.; Scrosati, B. *Adv. Mater.* **2010**, *22*, 5198–5201.
(5) Suo, L.; Hu, Y.-S.; Li, H.; Armand, M.; Chen, L. *Nat. Commun.* **2013**, *4*, 1481.
(6) Hayashi, A.; Ohtomo, T.; Mizuno, F.; Tadanaga, K.; Tatsumisago, M. *Electrochem. Commun.* **2003**, *5*, 701–705.
(7) Nagao, M.; Hayashi, A.; Tatsumisago, M. *J. Mater. Chem.* **2012**, *22*, 10015–10020.
(8) Yang, Y.; Zheng, G.; Cui, Y. *Chem. Soc. Rev.* **2013**, *42*, 3018–3032.
(9) Hayashi, A.; Ohtsubo, R.; Tatsumisago, M. *Solid State Ionics* **2008**, *179*, 1702–1705.
(10) Kobayashi, T.; Imade, Y.; Shishihara, D.; Homma, K.; Nagao, M.; Watanabe, R.; Yokoi, T.; Yamada, A.; Kanno, R.; Tatsumi, T. *J. Power Sources* **2008**, *182*, 621–625.
(11) Yamada, T.; Ito, S.; Omoda, R.; Watanabe, T.; Aihara, Y.; Agostini, M.; Ulissi, U.; Hassoun, J.; Scrosati, B. *J. Electrochem. Soc.* **2015**, *162*, A646–A651.
(12) Agostini, M.; Aihara, Y.; Yamada, T.; Scrosati, B.; Hassoun, J. *Solid State Ionics* **2013**, *244*, 48–51.
(13) Nagao, M.; Imade, Y.; Narisawa, H.; Watanabe, R.; Yokoi, T.; Tatsumi, T.; Kanno, R. *J. Power Sources* **2013**, *243*, 60–64.
(14) Kato, Y.; Hori, S.; Saito, T.; Suzuki, K.; Hirayama, M.; Mitsui, A.; Yonemura, M.; Iba, H.; Kanno, R. *Nature Energy* **2016**, *1*, 16030.
(15) Hu, Y.-S. *Nature Energy* **2016**, *1*, 16042.
(16) Bae, C. J.; Erdonmez, C. K.; Halloran, J. W.; Chiang, Y. M. *Adv. Mater.* **2013**, *25*, 1254–1258.
(17) Lin, Z.; Liu, Z.; Fu, W.; Dudney, N. J.; Liang, C. *Angew. Chem., Int. Ed.* **2013**, *52*, 7460–7463.
(18) Lin, Z.; Liu, Z.; Dudney, N. J.; Liang, C. *ACS Nano* **2013**, *7*, 2829–2833.
(19) Hakari, T.; Hayashi, A.; Tatsumisago, M. *Chem. Lett.* **2015**, *44*, 1664–1666.
(20) Wang, H. F.; Jang, Y. I.; Huang, B. Y.; Sadoway, D. R.; Chiang, Y. T. *J. Electrochem. Soc.* **1999**, *146*, 473–480.
(21) Li, J.; Murphy, E.; Winnick, J.; Kohl, P. A. *J. Power Sources* **2001**, *102*, 294–301.
(22) Palacín, M. R.; de Guibert, A. *Science* **2016**, *351*, 1253292.
(23) Srivastava, S.; Schaefer, J. L.; Yang, Z.; Tu, Z.; Archer, L. A. *Adv. Mater.* **2014**, *26*, 201–234.
(24) Tjong, S. C. *Adv. Eng. Mater.* **2007**, *9*, 639–652.
(25) Machida, N.; Maeda, H.; Peng, H.; Shigematsu, T. *J. Electrochem. Soc.* **2002**, *149*, A688–A693.
(26) Dudney, N. J.; Li, J. C. *Science* **2015**, *347*, 131–132.
(27) Nagao, M.; Hayashi, A.; Tatsumisago, M.; Ichinose, T.; Ozaki, T.; Togawa, Y.; Mori, S. *J. Power Sources* **2015**, *274*, 471–476.
(28) Rao, R. P.; Adams, S. *Phys. Status Solidi A* **2011**, *208*, 1804–1807.
(29) Boulineau, S.; Courty, M.; Tarascon, J.-M.; Viallet, V. *Solid State Ionics* **2012**, *221*, 1–5.
(30) Yubuchi, S.; Teragawa, S.; Aso, K.; Tadanaga, K.; Hayashi, A.; Tatsumisago, M. *J. Power Sources* **2015**, *293*, 941–945.
(31) Wu, F. X.; Kim, H.; Magasinski, A.; Lee, J. T.; Lin, H. T.; Yushin, G. *Adv. Energy Mater.* **2014**, *4*, 1400196.
(32) Altorfer, F.; Bührer, W.; Anderson, I.; Schärpf, O.; Bill, H.; Carron, P.; Smith, H. *Phys. B* **1992**, *180*, 795–797.
(33) Oh, D. Y.; Nam, Y. J.; Park, K. H.; Jung, S. H.; Cho, S. J.; Kim, Y. K.; Lee, Y. G.; Lee, S. Y.; Jung, Y. S. *Adv. Energy Mater.* **2015**, *5*, 1500865.
(34) Hayashi, A.; Ohtsubo, R.; Ohtomo, T.; Mizuno, F.; Tatsumisago, M. *J. Power Sources* **2008**, *183*, 422–426.
(35) Tatsumisago, M.; Mizuno, F.; Hayashi, A. *J. Power Sources* **2006**, *159*, 193–199.
(36) Han, F.; Zhu, Y.; He, X.; Mo, Y.; Wang, C. *Adv. Energy Mater.* **2016**, *6*, 1501590.
(37) Yang, Y.; Zheng, G.; Misra, S.; Nelson, J.; Toney, M. F.; Cui, Y. *J. Am. Chem. Soc.* **2012**, *134*, 15387–15394.
(38) Zhang, S. S. *J. Power Sources* **2013**, *231*, 153–162.

DOI: 10.1021/acs.nanolett.6b01754
Nano Lett. 2016, 16, 4521–4527

(39) Takeuchi, T.; Kageyama, H.; Nakanishi, K.; Tabuchi, M.; Sakaebe, H.; Ohta, T.; Senoh, H.; Sakai, T.; Tatsumi, K. *J. Electrochem. Soc.* **2010**, *157*, A1196−A1201.

DOI: 10.1021/acs.nanolett.6b01754
Nano Lett. 2016, 16, 4521−4527